

Revision 1

Coexisting hematite induces and accelerates the transformation of ferrihydrite: pathway and underlying mechanisms supplementary materials

Hongyan Wei^{1,2,3}, Jing Liu^{4*}, Qingze Chen^{1,2,3}, Yixuan Yang^{1,2,3}, Haiyang Xian^{1,2,3},
Xiaoliang Liang^{1,2,3}, Yiping Yang^{1,2,3}, Jianxi Zhu^{1,2,3}, Runliang Zhu^{1,2,3*}

1. CAS Key Laboratory of Mineralogy and Metallogeny/Guangdong provincial Key Laboratory of Mineral Physics and Materials, Guangzhou Institute of Geochemistry, Chinese Academy of Sciences (CAS), Guangzhou, 510640 China

2. CAS Center for Excellence in Deep Earth Science, Guangzhou 510640, China

3. University of Chinese Academy of Science, Beijing, 100049 China

4. State Key Laboratory of Lunar and Planetary Sciences, Macau University of Science and Technology, Taipa 999078, Macau, China

*Corresponding author

E-mail: jingliu@must.edu.mo (Jing Liu); zhurl@gig.ac.cn (Runliang Zhu)

Table of content

Text S1. The calculation procedure of the actual Hem and Gth contents via the k -value method.

Text S2. The calculation procedure of the theoretical Hem and Gth contents.

Text S3. The transformation of dried Fhy in the absence and presence of Hem nanoplates.

Table S1. The reflection area of Gth (110) (A_G) and Gth (130) and Hem (104) (A_{H+G}).

Table S2. The actual, theoretical, and induced Hem contents in the products with different Hem nanoplate contents.

Figure S1. Structure characteristics of Fhy and hexagonal Hem nanoplates.

Figure S2. SEM images of the original samples composed of Fhy and Hem at different pH.

Figure S3. The XRD patterns and the SEM images of Hem nanoplates before and after reacting under different conditions.

Figure S4. The theoretical and actual content of Hem in Fhy-20Hem after reacting at pH 4, pH 7, and pH 12 for 10 days.

Figure S5. The SEM images of Fhy-5Hem-4-10d and Fhy-70Hem-4-10d.

Figure S6. The TEM images of Hem nanoplates in Fhy-20Hem-4-10d and Fhy-20Hem-4-0d from the side view.

Figure S7. The SEM image of layer-by-layer growth and the TEM images of flower-like iron oxides with continuous lattice between the central Hem and the petal Gth at Fhy-20Hem-12-24h.

Figure S8. The XRD and SEM images of transformation products from the dried Fhy in the absence and presence of Hem nanoplates.

Figure S9. The XRD patterns and the SEM images of transformation products of Fhy in the presence of 70% Hem nanoplates at pH 12.

Text S1. The procedure of calculating the actual Hem and Gth contents via the k -value method

The contents of Hem and Gth are calculated by the k -value method based on the equation:

$$R_G = (A_G/K_G)/(A_G/K_G + A_H/K_H)$$

Where R_G is the ratio of Gth/(Gth + Hem), A_G is the area of (110) reflection of Gth, A_H is the area of (104) reflection of Hem, K_G , and K_H are the k -value of Gth and Hem that are normally taken as 2.79 and 3.26, respectively. The areas of Gth (110) and Hem (104) are acquired through the Jade 6 based on the reflections at 21.2° and 33.2° (shown in Table S1). The reflection at 21.2° represents the Gth (110), and the reflection at 33.2° is ascribed to the Gth (130) and Hem (104). We can calculate the area of Hem (104) based on the relation that the area of Gth (130) is about 36.4% of its (110). i.e.,

$$A_H = A_{(H+G)} - A_G * 0.364$$

Then, the Hem ratio is acquired through the $1-R_G$.

Text S2. The procedure of calculating the theoretical contents of Hem and Gth

The actual ratios of Hem and Gth in the pure Fhy systems could be calculated via the XRD data as ascribed in Text S1. The theoretical contents of Hem and Gth in Fhy-Hem systems would be calculated based on the actual contents of Hem and Gth in the pure Fhy samples. The procedures of calculating are described as follows. First, the molar content of Fhy is calculated through the equation:

$$n = m/M$$

Where m is the transformed mass of Fhy (we thought that the Fhy transformed completely when the residual Fhy contents were below 5%), M is the molar mass of Fhy which is taken as 107. Then the individual molar mass of Fhy transformed to Hem and Gth are calculated based on the contents of transformed Fhy and the contents of Hem and Gth in the final samples, which could be expressed by the equation:

$$(89 * x)/(160 * (n - x)) = R_G/R_H$$

Where x is the molar content of Fhy transformed to Gth, $89 * x$ and $160 * (n - x)$ represent the mass of Gth and Hem; R_G and R_H are the ratios of Gth and Hem calculated from the pure Fhy samples as described in Text S1. Next, the total mass (m_t) of crystalline minerals is calculated:

$$m_t = 89 * x + 160 * (n - x) + m_{Hem}$$

Where m_{Hem} is the added Hem nanoplate contents, and $160 * (n - x) + m_{Hem}$ represents the theoretical total mass of Hem. Finally, the theoretical contents of Gth and Hem are calculated via the equation:

$$R_T = m / m_t$$

Where R_T and m represent the theoretical ratio and mass of Gth or Hem.

Text S3. The transformation of dried Fhy in the absence and presence of Hem nanoplates

The synthesis of Fhy was carried out using a protocol based on previous studies, involving the rapid hydrolysis of $Fe(NO_3)_3 \cdot 9H_2O$ (Cornell and Schwertmann 2003). Specifically, a desired amount of 1 M $Fe(NO_3)_3 \cdot 9H_2O$ solution was titrated to pH 7-8 by 3 M NaOH under continuous magnetic stirring. Subsequently, the suspension was allowed to equilibrate for a period of approximately 2 h. All precipitates were washed four times with ultrapure water by centrifugation at 11000 rpm for 10 min and then freeze-dried, ground, and saved in a desiccator.

The hydrothermal transformation experiments were carried out in sealed 250 ml polypropylene bottles at a temperature of 75°C in a water bath, and the two bottles were labeled as Fhy or Fhy-20Hem. 2.4 g Fhy powder was respectively suspended in 100 ml ultrapure water within the two bottles, and 0.6 g Hem nanoplate nanoplates were added in the Fhy-20Hem systems. The pH of these suspensions was adjusted to 12 and stirred for 2 h before initiating the transformation at 75°C. The pH was not readjusted during these reactions. After hydrothermal reaction for 0, 2, 4, 8, 12, and 24 h, 15 ml of the suspensions were collected from the bottles and centrifuged at 11000 rpm for 10 min to remove the supernatant, and the resulting precipitates

were freeze-dried for XRD and SEM analysis.

The weaker reflection intensities of products as shown by XRD in dried Fhy samples compared with undried Fhy systems mean a slower transformation rate of dried Fhy (Fig. S7a and Fig. 1c), which can be ascribed to the lower dissolution rate of dried Fhy than that of undried Fhy (Lewis 1992). This phenomenon could demonstrate that the undried Fhy has a lower crystallinity and is easily dissolved to produce Fe^{3+} and further recrystallized to Gth. The faster transformation rate of undried Fhy indicated that more Fe^{3+} dissolved from Fhy at the same time compared with the dried Fhy. In addition, the weaker Gth reflections and stronger Hem reflections in XRD patterns in the presence of Hem nanoplates compared with the condition in the absence of Hem nanoplates demonstrated the induced transformation of Fhy to Hem by Hem nanoplates in dried Fhy systems (Fig. S7b), which is similar with the induced transformation behaviors observed in the undried Fhy in the presence of Hem nanoplates. The Gth reflections were even not observed in dried Fhy systems with Hem nanoplates (Fig. S7b). The SEM images show that the main product of dried Fhy transformation was Gth, and Hem particles were also observed (Fig. S7c), which were similar to the products in undried Fhy systems (Fig. 5e). In the presence of Hem heterogeneous surfaces, little Gth particles were observed in the SEM images, which is similar with the XRD results (Fig. S7a), while the newly formed single Hem particles were still observed (Fig. S7d). The SEM image also clearly shows that the Hem nanoplate grew through the layer-by-layer and the heteroepitaxial growth of Gth on Hem nanoplates was not observed in the dried Fhy system (Fig. S7d). As such, we can conclude that the lower transformation rate (i.e., low Fe^{3+} supply) of dried Fhy is not beneficial for the heteroepitaxial growth of Gth on Hem.

Table S1. The reflection area of Gth (110) (A_G) and Gth (130) and Hem (104) (A_{H+G}) from the XRD pattern.

samples	A_G	A_{H+G}	samples	A_G	A_{H+G}
Fhy-4-10d	25861	17905	Fhy-20Hem-4-10d	7602	40327
Fhy-7-10d	7403	22629	Fhy-20Hem-7-10d	5135	24384
Fhy-12-24h	31868	17913	Fhy-20Hem-12-24h	18788	28097

Table S2. The actual, theoretical, and induced Hem contents in the products with different Hem nanoplate contents.

	Fhy	Fhy-5Hem	Fhy-10Hem	Fhy-20Hem	Fhy-40Hem	Fhy-70Hem
Actual content (%)	25.4	35.4	49.0	67.6	91.7	100
Theoretical content (%)	-	29.4	33.3	41.1	56.4	78.6
Induced content (%)	-	6.0	15.7	26.5	35.3	>21.4

Figure S1. Structure characteristics of Fhy and hexagonal Hem nanoplates. SEM images and XRD pattern of (a) Fhy and (b) hexagonal Hem; (c) TEM image of a single crystal of hexagonal Hem lying flat, and (d) HRTEM image of Hem from the area indicated by the yellow square in c, and the inset shows the corresponding FFT pattern along the Hem [001] zone axis; The HRTEM image shows that the intersecting lines of the up and down-side edge facets are parallel to (110), ($\bar{1}$ 20), and ($\bar{2}$ 10).

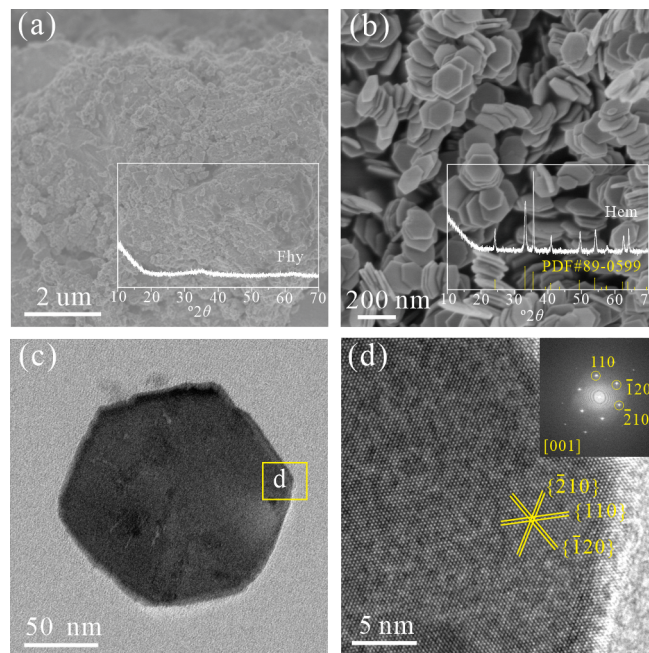


Figure S2. SEM images of the original samples composed of Fhy and Hem. **(a)** Fhy-20Hem-4, **(b)** Fhy-20Hem-7, **(c-d)** Fhy-20Hem-12, **(e)** Fhy-5Hem-4, **(f)** Fhy-70Hem-4. These samples are labeled as Fhy- x Hem- a , in which x and a represent the mass ratio of Hem nanoplate and pH, respectively (e.g., Fhy-20Hem-4 means that the sample with 20% Hem nanoplates before hydrothermal transformation at pH 4). The areas in yellow circles in b represent the small aggregates of Fhy dispersed by Hem nanoplates at pH 7.

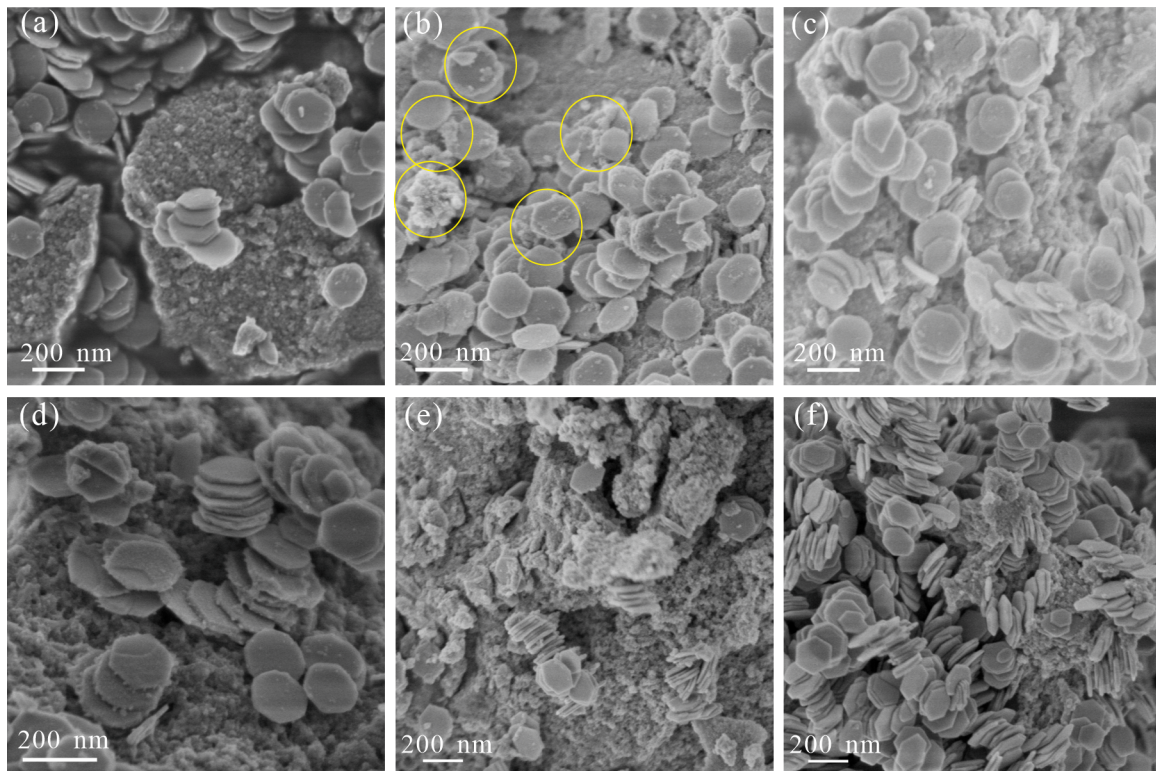


Figure S3. (a) The XRD patterns of the Hem nanoplates before and after reacting under different conditions.

The SEM images of (b) Hem nanoplates, (c) Hem-4-10d, and (d) Hem-12-24h, showing negligible changes

in the morphology after reacting under different conditions.

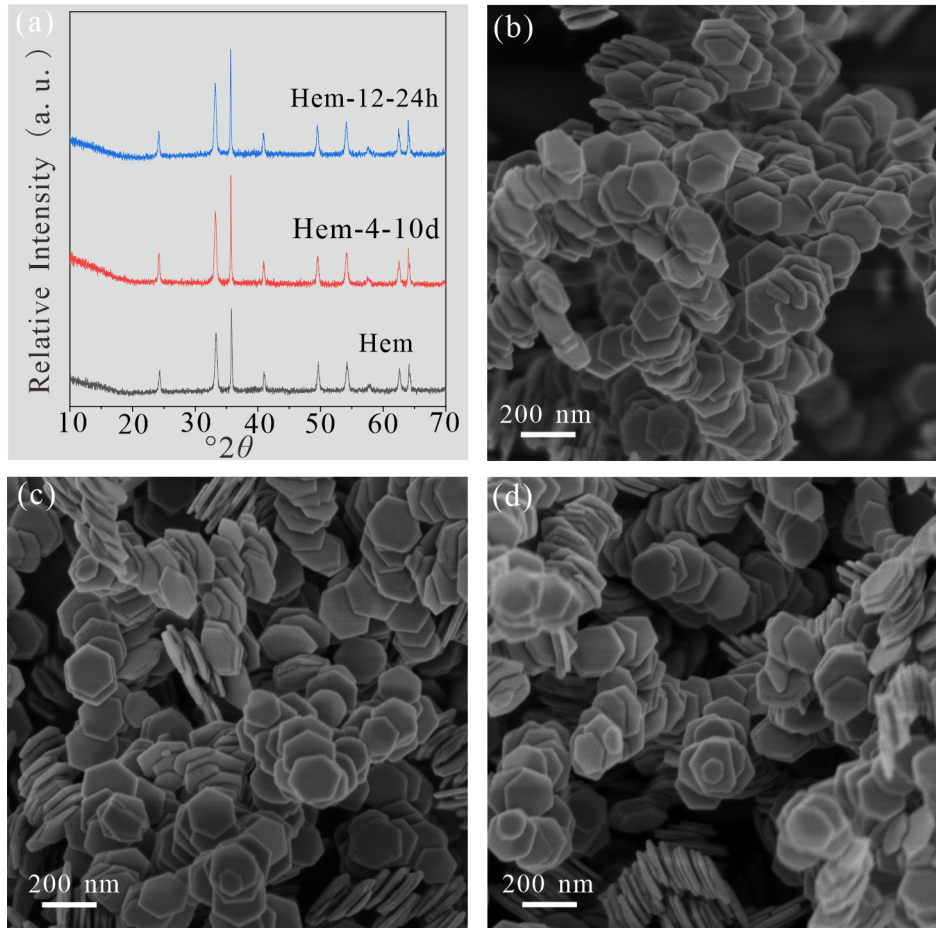


Figure S4. The theoretical and actual content of Hem in Fhy-20Hem after reacting at pH 4, pH 7, and pH 12 for 10 days based on (a) XRD and (b) Mössbauer spectra data.

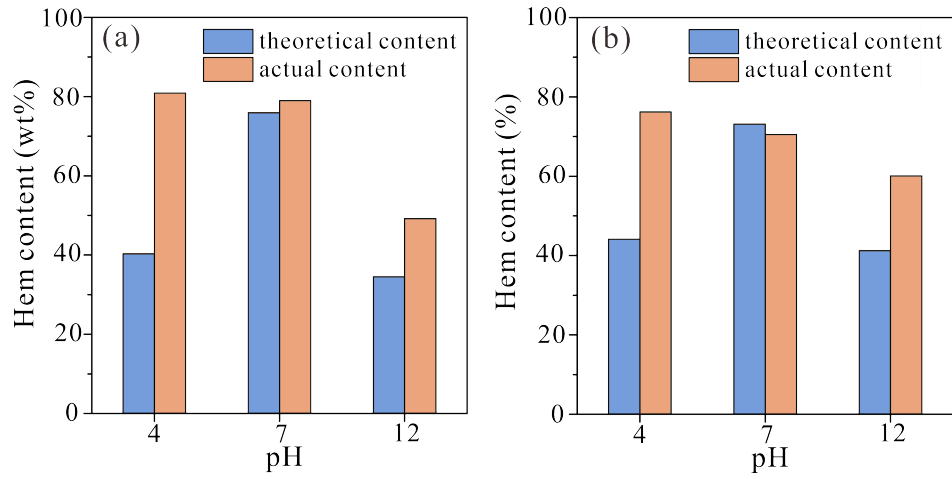


Figure S5. The SEM images of **(a)** Fhy-5Hem-4-10d, and **(b)** Fhy-70Hem-4-10d. The samples in red circles and yellow frames represent the island growth and layer-by-layer growth of Hem nanoplates, respectively.

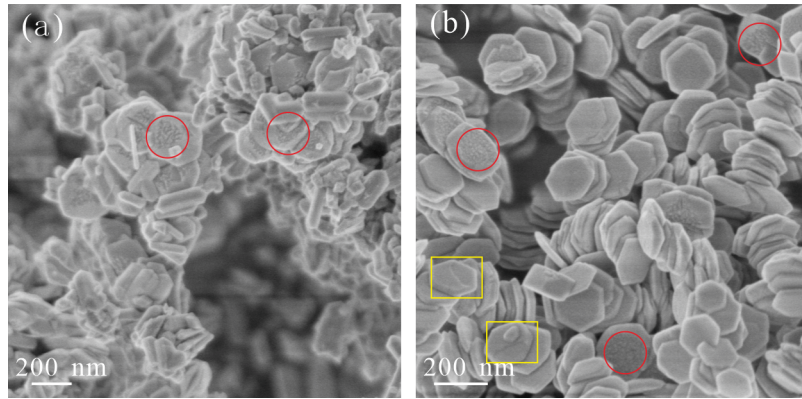


Figure S6. (a) The TEM image of Hem nanoplates in Fhy-20Hem-4-10d from the side view, (b) the TEM image of Hem in Fhy-20Hem-4-0d from the side view.

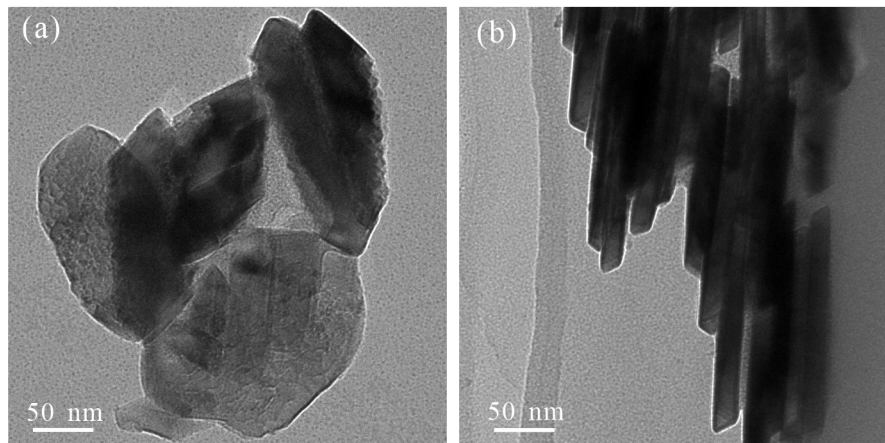


Figure S7. (a) The SEM image of layer-by-layer growth on the {001} facets of Hem nanoplates in Fhy-20Hem-12-24h. **(b)** The TEM image of flower-like iron oxides formed at pH 12, the center of the flower consisted of Hem, and the petals of the flower were composed of Gth. **(c)** HRTEM images of continuous lattice between the central Hem and the petal Gth.

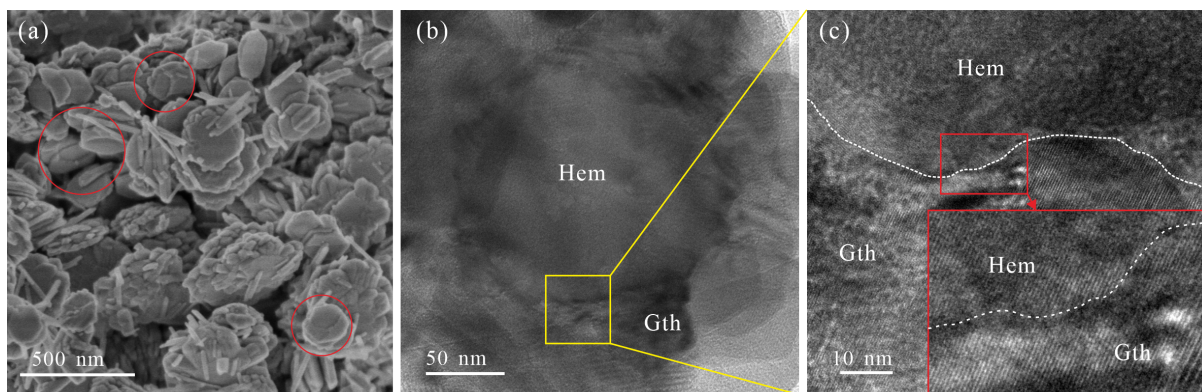


Figure S8. (a) XRD patterns recording the transformation process of dried Fhy at pH 12. (b) XRD patterns recording the transformation process of dried Fhy in the presence of Hem nanoplates at pH 12. (c) The SEM image of products formed from the dried Fhy. (d) The SEM image of products formed from the dried Fhy in the presence of Hem nanoplates.

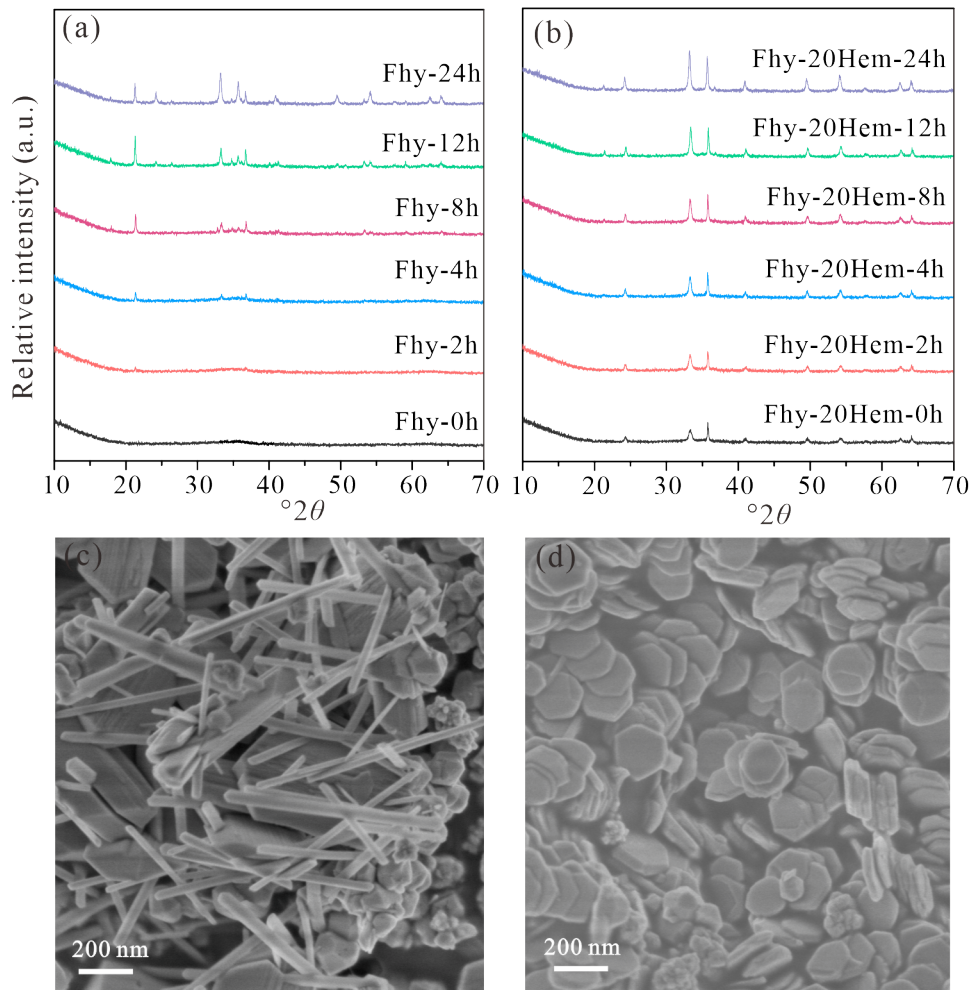
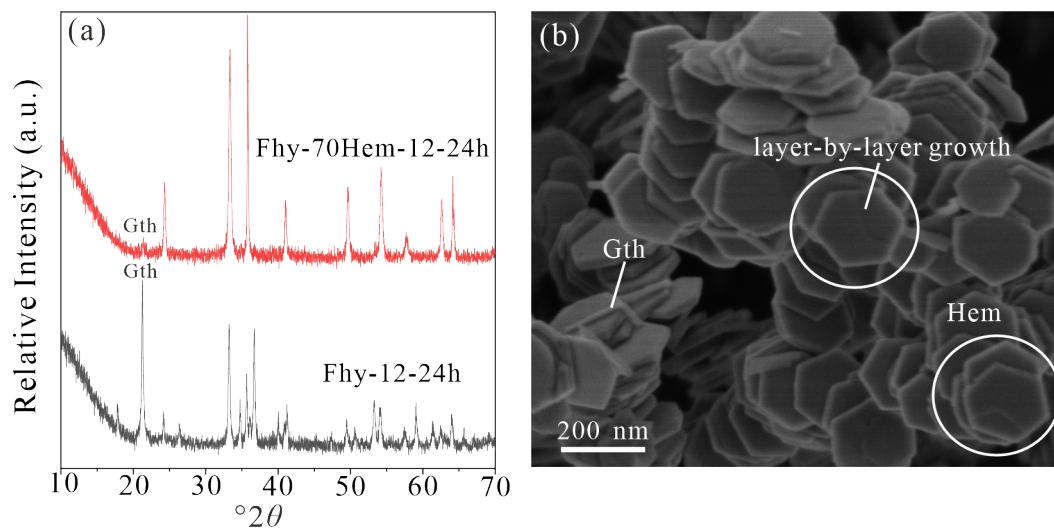


Figure S9. (a) XRD patterns recording the transformation products of Fhy reacted at pH 12 for 24 h in the absence/presence of 70% Hem nanoplates. (b) SEM image of the transformation products of Fhy-70Hem reacted at pH 12 for 24 h, showing the absence of heteroepitaxial growth of Gth.



References:

Lewis, D.G. (1992) Transformation induced in ferrihydrite by oven-drying. *Z. Pflanzenernähr. Bodenk.* **155**, 461-466.

Cornell, R.M., and Schwermann, U. (2003) *The iron oxides: structure, properties, reactions, occurrences and uses*. 2nd ed, Wiley-VCH.